IEEE Photonics Journal
An IEEE Photonics Society Publication

Open Access

Plasmonic Enhanced Optical Absorption in Organic Solar Cells With Metallic Nanoparticles

Volume 5, Number 4, August 2013

Fang Liu
Wanlu Xie
Qi Xu
Yuxiang Liu
Kaiyu Cui
Xue Feng
Wei Zhang
Yidong Huang

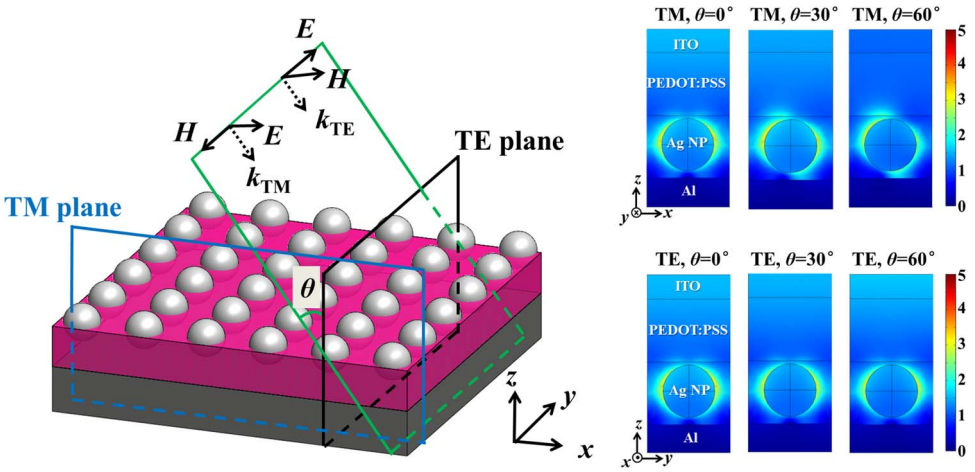

DOI: 10.1109/JPHOT.2013.2274767

IEEE photonics SOCIETY

IEEE

Plasmonic Enhanced Optical Absorption in Organic Solar Cells With Metallic Nanoparticles

Fang Liu, Wanlu Xie, Qi Xu, Yuxiang Liu, Kaiyu Cui, Xue Feng, Wei Zhang, and Yidong Huang

Department of Electronic Engineering, Tsinghua National Laboratory for Information Science and Technology, Tsinghua University, Beijing 100084, China

DOI: 10.1109/JPHOT.2013.2274767

Manuscript received June 4, 2013; revised July 15, 2013; accepted July 15, 2013. Date of publication July 26, 2013; date of current version August 9, 2013. This work was supported by the National Basic Research Programs of China (973 Program) under Contracts 2013CBA01704 and 2010CB327405, by the National High-Tech R&D Program (863 Program) under Contract 2011AA050504, and by the National Natural Science Foundation of China under Contracts NSFC-61036011, 61107050, and 60877023. Corresponding authors: F. Liu and Y. Huang (e-mail: liu_fang@tsinghua.edu.cn; yidonghuang@tsinghua.edu.cn).

Abstract: The plasmonic enhanced absorption of thin-film organic solar cell (OSC) with silver nanoparticles has been simulated and analyzed in the two-dimensional (2-D) and three-dimensional (3-D) simulation models by considering the position of nanoparticles inside the OSC and the incident angle and polarization of the incident light. It is found that, for TM polarization incidence, obvious optical absorption enhancement is obtained in both 2-D and 3-D cases. The absorption enhancement reaches more than 200% with nanoparticles deposited at the interface of PEDOT:PSS and P3HT:PCBM layer, which is larger than that with nanoparticles inside the active layer. However, for TE polarization incidence, the optical absorption is worsened rather than enhanced with metal nanostructures in the 2-D model, which is different with the results derived in the 3-D model. The absorption enhancement characteristics are also studied at oblique incidence, and the high absorption enhancement as high as 160% can be also obtained *when* the incident angle is increased to 60° in the 3-D model. By analyzing the mode profile in different circumstances, it could be concluded that the localized surface plasmon plays a significant role on improving the light absorption enhancement of OSC.

Index Terms: Plasmonic, surface plasmon polariton, organic solar cells, metallic nanoparticles.

1. Introduction

Surface plasmon polariton (SPP) is a kind of transverse-magnetic (TM) surface electromagnetic excitation that propagates in a wavelike fashion along the interface between metal and dielectric medium [1]. Due to the interaction between the electrons and electromagnetic field, the light can be trapped surrounding the metal nanoparticles (NPs) as the localized surface plasmon (LSP) mode [2]. It is demonstrated that the metal NPs could greatly enhance the light absorption of solar cells [3]–[8]. And this enhancement is much more significant for organic solar cell (OSC) with low light absorption capacity [5], [9], [10].

Although there are some studies analyzing the enhancement effect of the metal NPs in solar cells [11]–[14], just considering the normal incident light, one polarization, the two-dimensional (2-D) model and the fixed position of metal NPs in OSC cannot reveal the actual situation and the ability of light

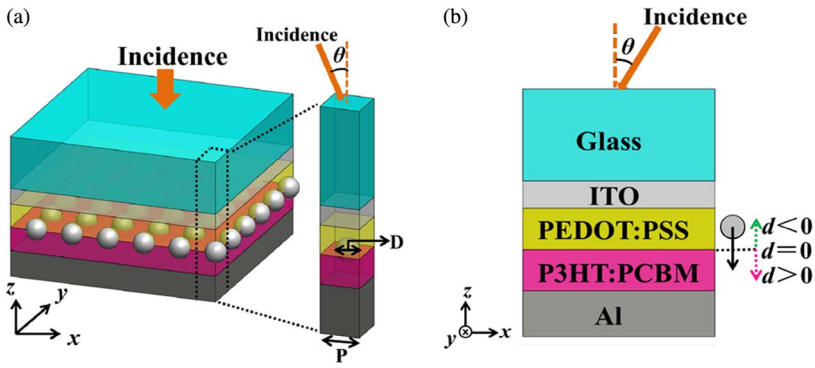

Fig. 1. Schematic diagram of thin film OSC with Ag NPs in (a) 3-D model and (b) 2-D model with incident angle θ. The d represents the distance between the center of Ag NPs and the interface of PEDOT:PSS and P3HT:PCBM.

absorption enhancement of metal NPs for OSC efficiency improvement. That is because the sunlight or indoor light would come into the active layer of OSC with different incident angle and polarization and the metal NPs would be separated in the different positions of OSC.

Recently, our group has shown that the location of metal NPs is related to the light absorption enhancement under normal incidence [10]. In this paper, the plasmonic enhanced light absorption in OSC has been further studied in both the 2-D and three-dimensional (3-D) models by considering the variation of light polarization and incident angle (θ), as well as the position of metal NPs. It is found that for TM polarized incidence $(\mathrm{TM_{in}})$, the optical absorption enhancement effect has little difference by using the 2-D and the 3-D models. Nevertheless, for TE polarized incidence $(\mathrm{TE_{in}})$, the light absorption is enhanced obviously in the 3-D model, but decreased dramatically in the 2-D model. The detailed analysis indicates that, to analyze the metal NPs enhanced light absorption characteristics under the $\mathrm{TE_{in}}$, the 3-D model should be adopted. Simulation results show that the light absorption enhancement as high as 200% could be derived at normal incidence when metal NPs locating at the interface of PEDOT:PSS and P3HT:PCBM layer. And the absorption enhancement effect is effective at not only vertical but also oblique incidence. The enhancement is still as high as 160% even when $\theta = 60^\circ$ in the 3-D model, which must be beneficial to OSC under sunlight with changing incident angles. The detailed analysis would help us to understand how metal NPs improve the light absorption of OSC.

2. Simulation Model and Method

The 3-D and 2-D simulation models of plasmonic enhanced OSC with Ag NPs are shown in Fig. 1(a) and (b), respectively. The OSC consists of the layers of glass substrate, indium tin oxide (ITO), poly(3,4-ethylenedioxythiophene):poly(styrenesulfonate) (PEDOT:PSS), poly(3-exylthiophene):(6,6)-phenyl-C61-butyric-acid-methylester (P3HT:PCBM), and aluminum (Al) cathode, whose thickness is assumed as 20 nm, 30 nm, 30 nm, and 100 nm, respectively. The active layer is P3HT:PCBM shown as the red layer in Fig. 1. A layer of periodic Ag NP array with diameter $(D = 25\ \mathrm{nm})$ and period $(P = 45\ \mathrm{nm})$ is located in the OSC with an offset distance (d) from the interface of PEDOT:PSS and P3HT:PCBM layer. The orientation of the square lattice of nanoparticles is along x and y axis. Here, $d = 0$ nm means the center of Ag NPs is just at the interface of PEDOT:PSS and P3HT:PCBM layer. The wavelength-dependent dielectric constants of ITO, PEDOT:PSS, P3HT:PCBM, Ag, and Al are the same with those in [15]–[17]. The refractive index of glass substrate is fixed as 1.46.

The finite element method (FEM) is used for numerical simulation with the help of the software package COMSOL Multiphysics [18]. A polarized plane wave (p wave or s wave) with wavelength λ_0, power P_{in}, and wave vector $\vec{k}$ is set as the input and propagates along the $-z$ direction with different incident angles $\theta(= 0^\circ, 30^\circ, \text{and } 60^\circ)$. The wave vector of incident light changes in z–x plane.

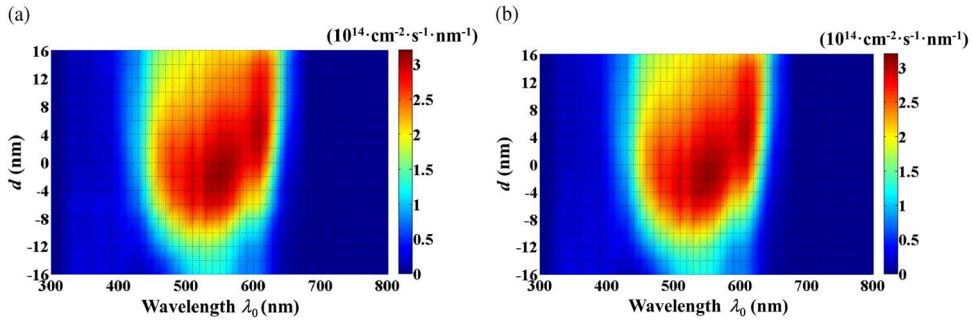

Fig. 2. The photon absorption spectrum of OSC embedded with Ag NPs as functions of wavelength and d in the 3-D model with (a) TM_{in} and (b) TE_{in} at normal incidence.

Here, p wave and s wave are also called TM and TE wave, respectively. For a certain incident wavelength, the distribution of electromagnetic field $(\boldsymbol{E}, \boldsymbol{H})$ inside the OSC could be obtained by solving the Maxwell equations. Here, to reduce the computational complexity, just one period of the structure is calculated by imposing the Floquet periodic boundary conditions in x and y directions (or only x direction in the 2-D model) as described in Ref. [19].

The absorbed light in the active layer (excluding the Ag NPs) is calculated according to [20]

$$\frac{1}{2}\omega\varepsilon_0 \int_V \mathrm{Im}[\varepsilon(\lambda_0)]|\boldsymbol{E}|^2 dV, \tag{1}$$

where ω is the angular frequency of incident light, V is the volume of the active layer, ε_0 is the permittivity in free space, and $\varepsilon(\lambda_0)$ is the complex dielectric constant of the active layer. The absorption rate $AR(\theta, \lambda_0)$ related to the incident angle and wavelength is defined as

$$AR(\theta, \lambda_0) = \frac{\frac{1}{2}\omega\varepsilon_0 \int_V \mathrm{Im}[\varepsilon(\lambda_0)]|\boldsymbol{E}|^2 dV}{P_{in}}. \tag{2}$$

The photon absorption number can be given as

$$AN_{\mathrm{AM1.5G}}(\theta, \lambda_0) = N_{\mathrm{AM1.5G}}(\lambda_0) \times AR(\theta, \lambda_0), \tag{3}$$

where $N_{\mathrm{AM1.5G}}(\lambda_0)$ is the photon flux of AM 1.5G [10]. Then the total absorption rate $(A_{\mathrm{AM1.5G}})$ at certain incident angle θ can be calculated as

$$A_{\mathrm{AM1.5G}}(\theta) = \frac{\int AN_{\mathrm{AM1.5G}}(\theta, \lambda_0) d\lambda_0}{\int N_{\mathrm{AM1.5G}}(\lambda_0) d\lambda_0}, \tag{4}$$

and the light absorption enhancement (AE) of OSC with NPs is defined as

$$AE = \frac{A_{\mathrm{AM15G}}(\theta) \text{ with NPs}}{A_{\mathrm{AM1.5G}}(0^\circ) \text{ without NPs}} \times 100\%. \tag{5}$$

It should be noticed in Eq. (5) that the absorption rate at oblique incidence is compared with that of normal incidence.

3. Results of the 3-D Model

First, the plasmonic enhancement effect of metal NPs on the OSC in the 3-D model, as shown in Fig. 1(a), is simulated. The angle and polarization of the incident light and the position of Ag NPs are varied to study how the metal NPs improve the light absorption of the OSC.

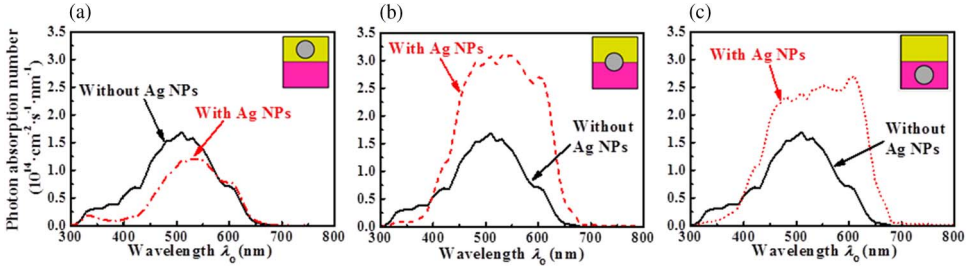

Fig. 3. Fixing d as $d = -14$ nm, $d = 0$ nm and $d = 14$ nm in Fig. 2, the photon absorption spectrum of OSC with Ag NPs located (a) inside the PEDOT:PSS, (b) at the interface PEDOT:PSS and P3HT:PCBM layers, and (c) inside the P3HT:PCBM is shown as the red lines, respectively. The black solid line indicates the photon absorption spectrum of OSC without Ag NPs.

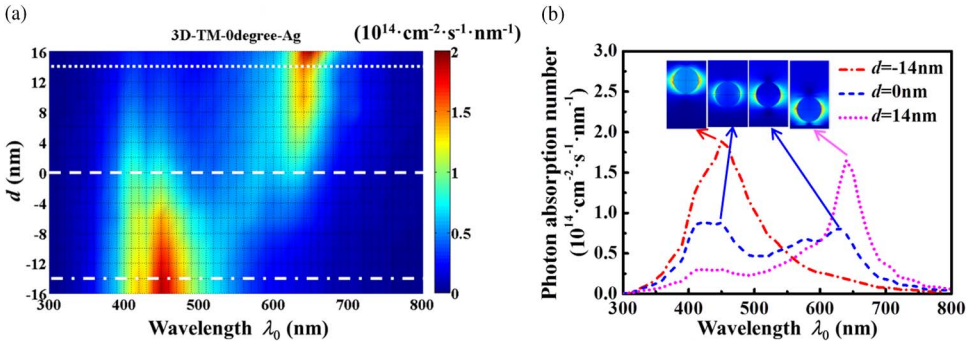

Fig. 4. (a) The photon number absorbed by Ag NPs as functions of wavelength and d at normal incidence of TM_{in} in the 3-D model. (b) Fixing d as the three white lines in (a), the photon absorption spectrum of Ag NPs is derived when $d = -14$ nm, $d = 0$ nm, and $d = 14$ nm corresponding to the red dot-dashed line, the blue dashed line and the pink dotted line, respectively. The insets show that the LSP mode is excited for each peak of the curves.

Fig. 2 shows the photon absorption number of OSC as functions of wavelength λ_0 and position of metal NPs d under normal incidence $(\theta = 0^\circ)$ of both TM and TE polarization. Considering the light absorption spectrum of OSC [21], the wavelength range from 300 nm to 800 nm is calculated here. The identical results shown in Fig. 2(a) and b) ascribe to the equivalent situation for TE and TM polarization in the 3-D model under normal incidence. Fixing d as -14 nm, 0 nm, and 14 nm, the photon absorption spectrum $AN_{AM1.5G}(0^\circ, \lambda_0)$ of OSC is shown as the red line in Fig. 3(a)–(c), respectively. Comparing with the light absorption of OSC without Ag NPs (shown as the black solid line), the Ag NPs have a bad effect on the light absorption of OSC when embedded inside the PEDOT:PSS layer $(d = -14$ nm$)$. And the Ag NPs improve the light absorption obviously when located inside $(d = 14$ nm$)$ and especially at the interface $(d = 0$ nm$)$ of the P3HT:PCBM active layer.

The AE with Ag NPs at the interface of PEDOT:PSS and P3HT:PCBM layer $(d \approx 0)$ is even higher than that with Ag NPs inside the P3HT:PCBM layer $(d \approx 14$ nm$)$. The previous study indicated that the light trapping induced by the LSP mode dominates the light absorption enhancement with metal NPs [10], and the electric field of LSP mode inside the metal NPs is proportional to that outside [10], [22]. Therefore, the light absorbed inside the Ag NPs, revealing most of the light trapped and absorbed by the active layer of OSC, is calculated to help us understand the influence of position of Ag NPs on improving the light absorption.

Taking the 3-D model with TM_{in} at 0° incidence for example, Fig. 4(a) illustrates the photon absorbed by the Ag NPs rather than the OSC, which reflects the enhanced light absorption due to LSP mode. It is shown that there exist two strong photon absorption regions (one is from 400 nm to 500 nm when $d < 5$ nm and the other one is from 625 nm to 675 nm when $d > -5$ nm). Fixing d as -14 nm, 0 nm, 14 nm, the photon absorption spectrum is shown in Fig. 4(b), and only one

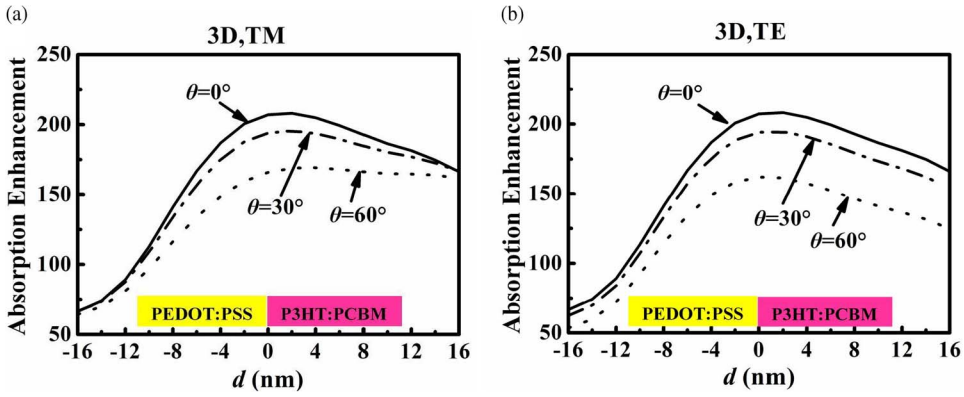

Fig. 5. The absorption enhancement as a function of the offset d in the 3-D model under (a) TM_{in} and (b) TE_{in} at different incident angles $(\theta = 0°, 30°, 60°)$.

absorption peak is excited when $d = -14$ nm and $d = 14$ nm. Since the light trapping in the PEDOT:PSS layer has no help for converting light to electricity, the *AE* is not only improved but also worsened with Ag NPs embedded inside PEDOT:PSS layer. When Ag NPs are located at the interface of PEDOT:PSS and P3HT:PCBM layer $(d = 0$ nm$)$, the optical absorption enhancement can occur at both long and short wavelength region, which results in the largest *AE*. The two absorption peaks should be attributed to the contact of two different materials (PEDOT:PSS and P3HT:PCBM) with Ag NPs, and the LSP mode is excited at different wavelength shown as the insets of Fig. 4(b).

By integrating the photon absorption numbers with respect to the wavelength in Fig. 2, the total absorption rate of OSC with Ag NPs can be obtained according to Eq. (4). And the *AE* varying with d at normal incidence can be derived with Eq. (5). The results are shown by the solid lines in Fig. 5(a) and (b), respectively. The maximum *AE* reaches up to 217% when d is about 2 nm.

Furthermore, the incident angle θ is varied as 30° and 60° to check whether the high *AE* can still be obtained at oblique incidence. This is an important issue for the actual applications of solar cells, because the light mostly comes into the solar cells at oblique incidence. The dash-dotted line and dotted line in Fig. 5 illustrate that, for TM_{in} and TE_{in}, the Ag NPs also have significant light absorption enhancement to the OSC and the maximum value of *AE* is about 190% $(\theta = 30°)$ and 170% $(\theta = 60°)$, respectively. The results indicate that Ag NPs can enhance absorption at different incident angles by selecting proper position of metal NPs.

To understand this light absorption enhancement, the electric field intensity distributions in the OSC should be observed. Considering the polarization of the incident light, the TM plane and TE plane shown in Fig. 6(a) is defined. It is shown in Fig. 6(b) and (c) that the LSP mode has been excited in both TM_{in} and TE_{in} circumstances resulting in the *AE* enhancement even at oblique incidence.

For TE_{in} shown in Fig. 6(c), the field of LSP mode under TE_{in} remains the same with different θ. Since the OSC consists of five layers, the transmission and reflection at the interfaces of these layers are somewhat different for different incidence. For this reason and the definition of Eq. (5), although the LSP mode field distribution is the same for different incident angles, the enhancement is less for oblique incident comparing to normal incidence. But for TM_{in} shown in Fig. 6(b), the field direction of LSP mode changes with θ. In the view of LSP mode, the Ag NPs become closer to the interface of PEDOT:PSS and P3HT:PCBM layer at large θ which leads to larger *AE* compared with that with TE_{in}. Thus, at oblique incidence, the *AE* with TM_{in} becomes higher than that with TE_{in} when $d > 0$ nm, especially when Ag NPs are totally deposited in the active layer $(d \approx 14$ nm$)$.

4. Results of the 2-D Model

Although the 3-D model reveals the real situation, the 2-D model can greatly simplify the complexity of calculation and has been adopted to guide experimental design. Thus, it is necessary to simulate

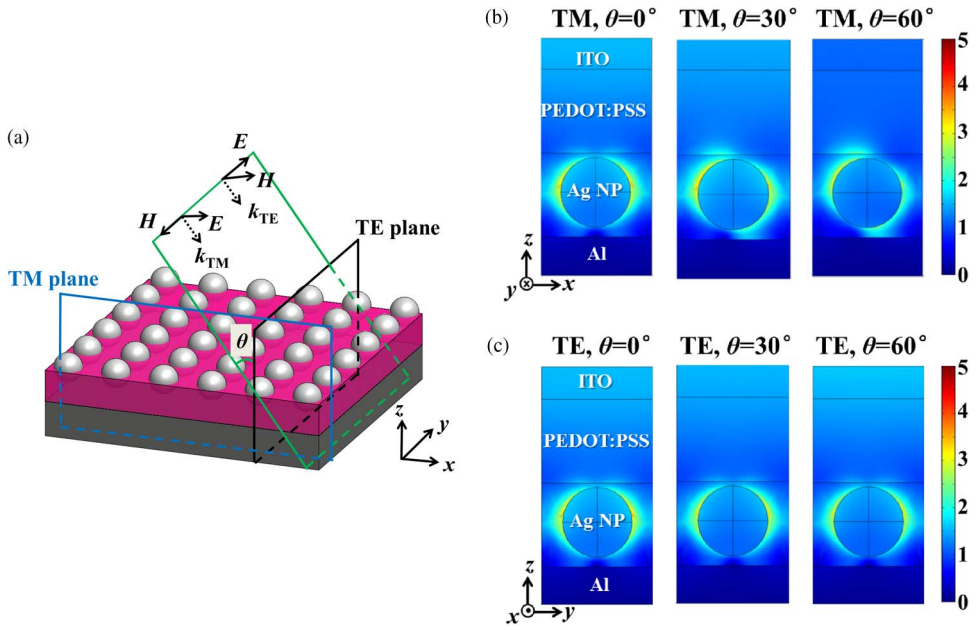

Fig. 6. (a) Schematic diagram of the OSC under TM and TE polarized incidence. The TM (TE) plane is defined as the x–z plane (y–z plane) crossing the center of a group of NPs. The electric field intensity distribution of the OSC with Ag NPs embedded inside the active layer ($d = 14$ nm) under (b) TM_{in} and (c) TE_{in} at 0°, 30°, 60° incidence ($\lambda_0 = 500$ nm) in the 3-D model.

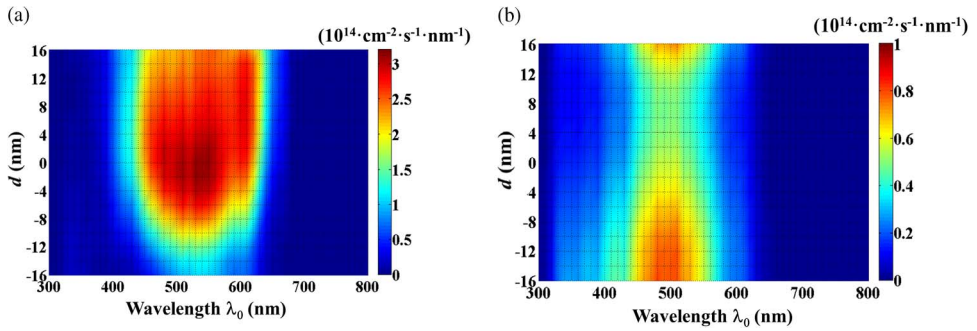

Fig. 7. In the 2-D model, the photon absorption spectrum of OSC with Ag NPs as functions of wavelength and d for normal incidence of (a) TM_{in} and (b) TE_{in}.

the absorption performance of OSC in the 2-D model and compare it with that derived in the 3-D model.

For the 2-D model, the periodic metal nanostructure remains in x–z plane, but the structure keeps invariant along y axis. Fig. 7(a) and (b) shows the photon absorption spectrum $AN_{AM1.5G}(\theta = 0, \lambda)$ of OSC under TM_{in} and TE_{in}, respectively. It is shown that the spectrum is similar for 2-D and 3-D model under TM_{in}. However, under TE_{in}, the light absorption of OSC shown in Fig. 7(b) is much different from Fig. 2(b) and decreased dramatically in the 2-D model with the strongest value just 1/3 of the TM case. The reason can be known by taking a look at the field intensity distribution in the OSC.

Fig. 8(a) illustrates that, for the TM_{in}, the LSP mode is excited obviously surrounding the Ag NP with enhanced field. While for the TE_{in}, no LSP mode can be observed and most of the light cannot even propagate into the active layer (P3HT:PCBM) as shown in Fig. 8(b). This is because that the NPs in fact become nano-cylinders in the 2-D model with periodic nanostructure along x axis and invariant structure along y axis. The electric field of TM incidence along x axis could feel the

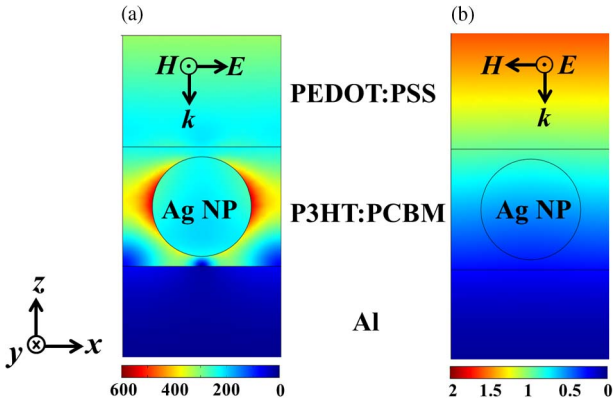

Fig. 8. Electric field intensity distribution of the OSC with Ag NPs embedded inside the active layer ($d = 14$ nm) under (a) TM_{in} and (b) TE_{in} when $\lambda_0 = 500$ nm and $\theta = 0^\circ$ in the 2-D model.

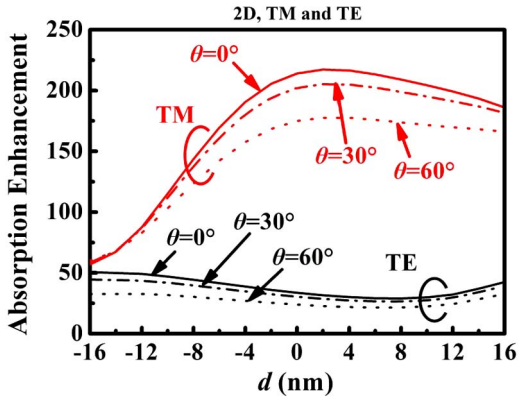

Fig. 9. The absorption enhancement as a function of the offset d in the 2-D model with TM_{in} (the red lines) and TE_{in} (the black lines) at different angles (0°, 30°, 60°).

nanostructures and excite the enhanced field of LSP mode, which greatly enhances the light absorption of OSC. However, for TE_{in}, the electric field is along y axis and could not excite the LSP mode. And the Ag nanostructures might even prevent the light come into the active layer of OSC and result in the bad effect on the light absorption of OSC.

Similar to Fig. 5 of the 3-D model, the AE as a function of d is shown in Fig. 9 with different polarization and incident angles. The red lines in Fig. 9 illustrate that the Ag NPs also have significant light absorption enhancement to the OSC for TM_{in}. Even for oblique incidence, the maximum value of AE is about 205% ($\theta = 30^\circ$) and 177% ($\theta = 60^\circ$) at $d \approx 2$ nm, respectively. The results indicate that Ag NPs can enhance light absorption at different incident angles by selecting proper position of metal NPs for TM_{in}. However, for TE_{in}, the black dash-dotted line and dotted line in Fig. 9 are even lower than the black solid line, which means there is no enhancement for TE_{in} at any incident angle. Therefore, to study the light absorption enhancement of metal NPs under TE_{in}, 3-D model rather than 2-D model should be adopted.

For the above simulation, the thickness of active layer P3HT:PCBM is fixed as 30 nm. While for thicker active layer, the light absorption enhancement would be not so significant. Taking the 2-D model with TM_{in} at normal incident for example, as shown in Fig. 10, the absorption enhancement drops dramatically when the thickness of active layer increases to more than 70 nm. Nevertheless, in actual metal NPs enhanced OSCs, there may be not just one layer of NPs existing in (or at the interface) the active layer and the metal NPs may not be located periodically as shown in Fig. 1.

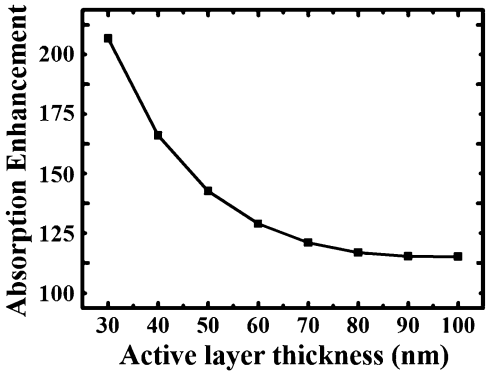

Fig. 10. Absorption enhancement as a function of the thickness of active layer (P3HT:PCBM) in the 2-D model with TM_{in} at normal incident and $d = 0$.

Thus, understanding the mechanism of light absorption enhancement with metal NPs, knowing the trend of enhancement varying with incident light and structure parameters, and mastering the simulation model in different circumstances are the key issues to be dealt with in this paper.

5. Conclusion

The optical absorption enhancement of thin film OSC with Ag NPs has been studied theoretically in the 2-D and 3-D model, where the polarization and incident angle of the input light and the position of NPs in the OSC are considered. It is found that the 2-D model is available for TM incidence, but the 3-D model should be adopted for TE incidence since the 2-D model gets an incorrect result. The simulation results indicate that the Ag NPs could greatly improve the light absorption of OSC under both TM and TE incidence based on the light trapping of LSP mode. By varying the position of Ag NPs inside the OSC, the maximum light absorption enhancement as high as 200% is obtained when depositing the Ag NPs near to the interface of anode layer (PEDOT:PSS) and active layer (P3HT:PCBM) rather than inside the active layer, which results from the wavelength range extension of LSP mode enhancement. At oblique incidence, the light absorption enhancement can also be derived and is about 160% even increasing the incident angle to 60°.

References

[1] H. Raether, *Surface Plasmons*. Berlin, Germany: Springer-Verlag, 1988, pp. 4–13.
[2] A. V. Zayats, I. I. Smolyaninov, and A. A. Maradudin, "Nano-optics of surface plasmon polaritons," *Phys. Rep.*, vol. 408, no. 3/4, pp. 131–314, Mar. 2005.
[3] H. A. Atwater and A. Polman, "Plasmonics for improved photovoltaic devices," *Nat. Mater.*, vol. 9, no. 3, pp. 205–213, Mar. 2010.
[4] K. Nakayama, K. Tanabe, and H. A. Atwater, "Plasmonic nanoparticle enhanced light absorption in GaAs solar cells," *Appl. Phys. Lett.*, vol. 93, no. 12, pp. 121904-1–121904-3, Sep. 2008.
[5] J. Yang, J. You, C. Chen, W. C. Hsu, H. Tan, X. Zhang, Z. Hong, and Y. Yang, "Plasmonic polymer tandem solar cell," *ACS NANO*, vol. 5, no. 8, pp. 6210–6217, Aug. 2011.
[6] D. Qu, F. Liu, J. Yu, W. Xie, Q. Xu, X. Li, and Y. Huang, "Plasmonic core-shell gold nanoparticle enhanced optical absorption in photovoltaic devices," *Appl. Phys. Lett.*, vol. 98, no. 11, pp. 113119-1–113119-3, Mar. 2011.
[7] Q. Xu, F. Liu, W. Meng, and Y. Huang, "Plasmonic core-shell metal-organic nanoparticles enhanced dye-sensitized solar cells," *Opt. Exp.*, vol. 20, no. 23, pp. A898–A907, Nov. 2012.
[8] X. Chen, B. Jia, J. K. Saha, B. Cai, N. Stokes, Q. Qiao, Y. Wang, Z. Shi, and M. Gu, "Broadband enhancement in thin-film amorphous silicon solar cells enabled by nucleated silver nanoparticles," *Nano Lett.*, vol. 12, no. 5, pp. 2187–2192, May 2012.
[9] J. B. Khurgin, G. Sun, and R. A. Soref, "Practical limits of absorption enhancement near metal nanoparticles," *Appl. Phys. Lett.*, vol. 94, no. 7, pp. 071103-1–071103-3, Feb. 2009.
[10] D. Qu, F. Liu, X. J. Pan, W. L. Xie, Q. Xu, and Y. D. Huang, "Mechanism of optical absorption enhancement in thin film organic solar cells with plasmonic metal nanoparticles," *Opt. Exp.*, vol. 19, no. 24, pp. 24 795–24 803, Nov. 2011.
[11] K. R. Catchpole and A. Polman, "Plasmonic solar cells," *Opt. Exp.*, vol. 16, no. 26, pp. 21 793–21 800, Dec. 2008.
[12] Y. A. Akimov, W. S. Koh, and K. Ostrikov, "Enhancement of optical absorption in thin-film solar cells through the excitation of higher-order nanoparticle plasmon modes," *Opt. Exp.*, vol. 17, no. 12, pp. 10 195–10 205, Jun. 2009.

[13] M. Yang, Z. Fu, F. Lin, and X. Zhu, "Incident angle dependence of absorption enhancement in plasmonic solar cells," *Opt. Exp.*, vol. 19, no. Suppl. 4, pp. A763–A771, Jul. 2011.
[14] L. Yang, Y. Xuan, and J. Tan, "Efficient optical absorption in thin-film solar cells," *Opt. Exp.*, vol. 19, no. Suppl. 5, pp. A1165–A1174, Sep. 2011.
[15] H. Hoppe, N. S. Sariciftci, and D. Meissner, "Optical constants of conjugated polymer/fullerene based bulk-heterojunction organic solar cells," *Mol. Cryst. Liq. Cryst.*, vol. 385, no. 1, pp. 113–119, Jan. 2002.
[16] F. Monestier, J. Simon, P. Torchio, L. Escoubas, F. Flory, S. Bailly, R. Bettignies, S. Guillerez, and C. Defranoux, "Modeling the short-circuit current density of polymer solar cells based on P3HT:PCBM blend," *Sol. Energy Mater. Solar Cells*, vol. 91, no. 5, pp. 405–410, Mar. 2007.
[17] E. D. Palik, *Handbook of Optical Constants of Solids*. Orlando, FL, USA: Academic, 1985.
[18] [Online]. Available: http://www.comsol.com/
[19] G. Veronis, R. W. Dutton, and S. Fan, "Metallic photonic crystals with strong broadband absorption at optical frequencies over wide angular range," *J. Appl. Phys.*, vol. 97, no. 9, pp. 093104-1–093104-4, May 2005.
[20] Y. A. Akimov and W. S. Koh, "Design of plasmonic nanoparticles for efficient subwavelength light trapping in thin-film solar cells," *Plasmonics*, vol. 6, no. 1, pp. 155–161, Mar. 2011.
[21] P. D. Cunningham and L. M. Hayden, "Carrier dynamics resulting from above and below gap excitation of P3HT and P3HT/PCBM investigated by optical-pump terahertz-probe spectroscopy," *J. Phys. Chem. C*, vol. 112, no. 21, pp. 7928–7935, May 2008.
[22] S. A. Maier, *Plasmonics: Fundamentals and Applications*. New York, NY, USA: Springer-Verlag, 2007.